Probabilistic Load Flow in AC Electrified Railways

T.K. Ho, Y.L. Chi, J. Wang, K.K. Leung, L.K. Siu and C.T. Tse

Abstract: System analysis within the traction power system is vital to the design and operation of an electrified railway. Loads in traction power system are often characterised by their mobility, wide range of power variations, regeneration and service dependence. Besides, the feeding systems may take different forms in AC electrified railways. Comprehensive system studies are usually carried out by computer simulation. A number of traction power simulators have been available and they allow calculation of electrical interaction among trains and deterministic solutions of the power network. In the paper, we present a different approach to enable load flow analysis on various feeding systems and service demands in AC railways by adopting probabilistic techniques. It is intended to provide a different viewpoint to the load condition. Simulation results are given to verify the probabilistic load flow models.

List of Symbols

I_t: train current

V_t: train voltage

$P_t + jQ_t$: train power

V_c: catenary voltage at a certain point

V_r: rail voltage at a certain point

V_s: voltage at the secondary winding of a feeding transformer

Z_s: source impedance

Z_c: self impedance on catenary (*c*) / unit length

Z_r: self impedance on rail (*r*) / unit length

Z_f: self impedance on feeder (*f*) / unit length

Z_{cr}: mutual impedance between catenary (*c*) and rail (*r*) / unit length

Z_{cf}: mutual impedance between catenary (*c*) and feeder (*f*) / unit length

Z_{rf}: mutual impedance between feeder (*f*) and rail (*r*) / unit length

V_{BT}: winding emf of a booster transformer

Z_{BT}: winding impedance of a booster transformer

1 Introduction

Traction power systems are physically huge electrical circuits with time-varying and moving loads. Power system analysis provides the necessary information for design, planning and operation. Simulation is commonly adopted as the most cost-effective tool for traction power studies. There are two major considerations in traction power simulation [1], namely accurate modelling of power networks and loads and efficient algorithms for solution. A number of traction power simulators have been developed [2-4] and they cover a wide range of applications and systems [5-7].

The traction power simulators usually include modelling of the track geometry and traction system characteristics and enable multi-train operations. By solving the power network equations, the simulators give details of electrical interactions among trains at specific time-steps over a long span of time and under different traffic conditions. Further enhancements have been introduced to improve the applicability and processing time [8-11]. For the purposes of design and planning, the loading conditions at the worst-case scenarios can be obtained through detailed traction power simulation. Together with appropriate design/safety margins from experience, system sizing or resilience study on the power system is possible.

In this study, an alternative approach, probabilistic load flow (PLF), is developed to investigate the loading conditions in the AC traction power systems. It has to be stressed that the traditional traction power simulators is not to be replaced by the PLF approach which is indeed intended to support and supplement those simulators. The outcome of the PLF study, probability density function (pdf) of voltage or power flow at certain point of the power system, indicates the ranges of variations of such parameters, hence the loading condition, on probabilistic basis with simple graphs, skipping the tedious process of extracting the required data from voluminous simulation results. PLF therefore provides a different viewpoint of insight into the system loading condition.

We present the application of probabilistic load flow in AC electrified railways and discuss the possible difficulties. The unique properties of the loads (trains) and the commonly adopted configurations of power feeding systems in railways are taken into consideration of the calculation. Even though the probability density functions (pdf's) of power, voltage and current at certain points in the network are generally not available from railway operators for

comparison, simulation results under various normal and extreme operational conditions are given to verify the methodology.

2 Power Load Flow

Load flow studies are the determination of the voltage, current, power, power factor and reactive power at various points in an AC electrical power system under existing or contemplated conditions of normal or extreme operation [12]. They provide vital knowledge of system dynamics of the existing set-up for system operation and maintenance, as well as the effects of interconnection with other power systems, and of new loads, generation stations and transmission line for future planning.

The scale of an electrified railway line is large enough to warrant substantial performance studies [13]. However, there are distinct operational differences between power system and railway traction power system. Because of the multiple sources (i.e. generators) in power system, the bus-bars are classified as slack, PV and PQ to ease convergence in the conventional load flow methods, such as Newton Raphson and Fast Decoupled and complicated algorithms are required to form the Jacobian matrix. In an AC traction system, there is only a single source in each feeding section (although there are always a number of feeding sections along a railway line). Whilst the loads in power systems are usually assumed to be of constant (or at least not fast-changing) MVA, the traction load is dynamic (dependent on train operation mode) and moving. The conventional methods are thus not as effective for load flow analysis in AC railways [14].

Power supplies for AC traction are obtained from the utility supply system, at transmission or sub-transmission voltage levels, through traction feeder substations. Different feeding systems are available, including direct supply with or without return conductors, booster transformer (BT) and autotransformer (AT) systems. A number of considerations, such as power transmission efficiency and interference suppression, have to be taken on the adoption of appropriate feeding system. The trains are the loads of the circuit and they are obviously not standing still. The power demand depends upon the train speed that in turn is related to a number of factors categorised by system specifications and operation conditions. The former includes traction equipment characteristics, track layout, signalling and speed restrictions whilst the latter covers the positions of trains, headway, traffic pattern and drivers' behaviour. As if it

were not complicated enough, a train might become a generator should regenerative braking be possible. Uncertainties of load demands are also common in typical power supply systems even though the extent is far less significant there. As a result, the increasing interest in probabilistic power-system design methods definitely applies to electrified railway system.

Probabilistic load flow (PLF) techniques were first developed [15] for DC models in power systems, followed by models for AC systems [16]. They provide a complete spectrum of all possible values of bus voltages, power flows and losses, with their respective probabilities, taking into account load uncertainties and control action effects. PLF has since found many successful applications [17-18].

Despite the numerous sources of uncertainties surrounding the load demand of a running train, the station-to-station runs, which usually include motoring toward the maximum allowable speed from one station, coasting if allowed, and braking to a halt for the next station, provide the much-needed pattern. This study first investigates the relationship between the station-to-station runs and their corresponding power demand and then devises the suitable probability density functions (pdf's) on which PLF starts. Different AC feeding systems in railways lead to different conductor layouts and current distribution, implying different approaches on load flow calculation. AT feeding involves the most complex current distribution. A simple model to support the necessary calculations for PLF analysis with AT feeding is presented here. The model is then extended to direct supply and BT feeding systems.

3 Supplies and Loads in AC Railways

To enable load flow analysis, it is necessary to have a thorough understanding of the two major components of the power supply network, the supply system and loads. AC railways are always prone to electromagnetic interference and some feeding systems are set up in such way that the return current is largely confined. Train, as a load, is on the move and their power demand and hence the effects on supply system depend on its operation and location. A relationship between power demand of a train and its mobility is crucial in load flow studies.

3.1 Feeding Systems

From power supply viewpoint, an AC railway line is divided into a number of feeding sections [13]. Adjacent sections are supplied by different phases and separated by neutral sections. A transformer substation is usually located at a certain position within each feeding section, supplying power to trains in the section. As a result, the supply network in one feeding section can be simply regarded as a single-source system.

Direct connection of the transformer secondary to the catenary and rails is the most straightforward means of power feeding. Significant rail-to-earth leakage current is the major drawback of this feeding arrangement because of the inevitable rail-to-earth impedance. The earth current is often one of the main causes of electromagnetic interference to the lineside telecommunication equipment, such as signalling circuitry. As shown in Fig. 1, the addition of a return conduction, in parallel with the catenary and connected to the rails at regular intervals, helps reduce the leakage current but only to a certain extent.

BT feeding provides another means of interference reduction by forcing the current to flow in the return conductor rather than in the rail. However, it is at the expense of poorer voltage regulation because of additional impedance of BTs. Having allowed power to be transmitted at the voltage twice as high as the operating voltage, AT feeding improves system efficiency. Interference suppression is another advantage of AT feeding. In addition, AT feeding provides better voltage regulation and allows longer interval between transformers [19], which is essential for service reliability of long-distance rail lines, if not just the capital cost. Both BTs and ATs are placed at regular intervals within a feeding section. Illustrated in Figs. 2 and 3, BT feeding system operates by balancing currents on the two windings of the transformers whilst AT feeding system relies on voltage balancing.

3.2 Loads

Train speed and operation mode are the decisive factors of the immediate amount of power required by the train as a load. They are however determined by the traction equipment characteristics, train weight, aerodynamics, track geometry and drive control. For an inter-station run, a train goes through different speeds and operation modes and the power demand may thus vary significantly within a short period of time. A simple and quick reference linking train speed and operation mode to the power required is essential to load flow calculation.

The fact that the trains are moving and carrying variable loads does not impose any difficulty on traction power system simulation [1] in which the details of power flow and energy consumption at every instant are available. In order to provide a general and simple picture of loading conditions in the system over a long span of time, load flow study is a simple and viable tool for any power system [12]. Given that the loads are moving with time-varying demands, a probabilistic approach is presented here to facilitate the load flow study. The number of trains in a feeding section is also vital to the calculation as they may be running at different speeds, drawing (or feeding) different amount of power from (or into) the feeding network and thus attributing different effects to the supply system. Nominal separation among trains is yet another important consideration and it should follow the timetables or headway of the train services.

4 Load Flow Calculation

One of the techniques for PLF is Monte Carlo simulation. The input parameters are induced by pseudo-random numbers and a large numbers of cases of load flows are probabilistically processed. Pdf's of power and voltage at selected points on the electrical network are the eventual outcomes. It is a very flexible method with plenty of successful applications [20] but it requires substantial computational effort. To alleviate the computational demand, assumptions will be introduced, particularly on the current distribution in various feeding systems, to simplify each load flow calculation. It must be noted that other methods of PLF [21-23] are also possible and valid and they may require different modelling on load conditions. Monte Carlo simulation is adopted here in order to provide a quick and reliable means for attaining the required pdf's and demonstrate the feasibility of PLF study in general.

4.1 Train Movement and Power Demand

With Monte Carlo simulation, there must be a primary random variable leading to the power required and its pdf should be readily available from random sampling. As train speed is related to power demand, it could have easily been taken as the primary random variable if it provided one-to-one mapping to power demand. From a typical train speed profile for an inter-station run, it can be deduced that the same train speed may imply not only difference in power demand, but also in power flow direction.

On the other hand, the train position, relative to the locations of the two stations of an inter-station run, is a useful indication of both operation mode and train speed. In an inter-station run, a train should be in motoring mode when it is close to the departing station whilst the brake must be on when the train is approaching the next station. With the easily attained speed profile, train speed and operation mode are directly identified by the train position. Thus, train position is used as the primary parameter in PLF calculation with Monte Carlo simulation.

For a given traction drive equipment, the characteristic curves from the manufacturers are used to estimate the power demand. If the train is in either motoring or (regenerative) braking mode, the tractive effort is obtained from the tractive-effort/speed characteristics of the train. The product between total tractive effort and train speed gives the necessary mechanical power output which in turn deduces the input electrical power from the efficiency/speed characteristics. Further, the power-factor/speed curve is used to devise reactive power. The train characteristic curves at nominal operation voltage are employed in this study. A set of characteristic curves at different voltages to cope with voltage variations certainly provides a more accurate model, at the expense of more computation time. Auxiliary power for the provision of air conditioning, lighting, doors and PA systems is included to the train power demand. 400kW of auxiliary power demand per train and a power factor of 0.9 are assumed.

A pdf of the train position has to be established before its random samples can be taken for further processing in load flow calculation. As the probability of a train being at a particularly position depends on the amount of time it spends on that position, it is therefore inversely proportional to the train speed. The position pdf is derived by the reciprocated inter-station speed profile (i.e. $1/speed$ vs distance), followed by normalising the area under the graph to one [24]. A typical train position pdf is shown in Fig. 4. Similar pdf's can then be obtained for different inter-station runs and/or operational conditions. Random samples are thus drawn from the resulting cumulative probability functions. For multi-station run, the speed profile over the stations is taken instead to generate the position pdf. The probability of the train waiting at stations (i.e. not requiring or generating power) is enhanced according to station dwell times.

On PLF study with more than one train on the track, the position of the first train is again generated from random sample of its position pdf. The subsequent trains are then located at a headway distance behind successively and their power demands are determined by their positions. Hence, the trains are at different stages of different inter-station runs, operating in

different modes and drawing/generating different amount of power. This approach allows different traffic conditions to be directly incorporated in load flow analysis while maintaining the flexibility of handling mixed traffic and/or headways along the line. It is also possible to add a stochastic factor in the headway to further represent small service perturbation. For example, the headway may be drawn from a normal distribution with mean at the nominal headway and a small standard deviation (say, 5% from the nominal).

4.2 AT Feeding

To facilitate load flow calculation, current distribution among the conductors in an AT feeding system is first defined and train voltage is expressed in term of its power demand. A single-train case, as illustrated in Fig. 5, is first considered as it enables simpler explanation of the model formulation. The discussion is then extended to cover the presence of multiple trains. The following assumptions are included to simplify the train voltage equations and hence reduce computational demand.

a) All conductors in an AT feeding system are reduced to the three main conductors – catenary (*c*), feeder (*f*) and rail (*r*), whilst others are merged into these three.
b) Self-impedance and mutual impedance of the conductors are treated as lumped parameters.
c) Rail-to-earth leakage current is small enough to be neglected.
d) Current flowing on the rails outside the two ATs supplying the train is small enough to be neglected.

(a) and (b) are acceptable simplifications to lessen computational demand without significantly jeopardising the overall accuracy [19]. (c) and (d) are simplified assumptions to enable demonstration of the load flow calculation. Detailed models can be applied here to include the rail-to-earth current and current in rails outside the two AT's enclosing the rails.

4.2.1 Single Train:

If the power demand of the train is $P_t + jQ_t$, train voltage $V_t = V_{tr} + jV_{ti}$ can be solved by a set of quadratic simultaneous equations according to the current distribution allowed by the AT feeding system.

$$V_{tr}^2 - V_s V_{tr} + Cot_r P_t + Cot_i Q_t + V_{ti}^2 = 0 \quad (1)$$

$$V_{ti} = \frac{Cot_r Q_t}{V_s} - \frac{Cot_i P_t}{V_s} \quad (2)$$

where V_s is the supply voltage and $Cot_r + jCot_i = Cot$ is a constant related to train position and self and mutual impedances of the conductors in the feeding system. Numerical methods, such

as Newton's method, can be employed to attain the solution of the non-linear simultaneous equations in a few iterations. Details of the equation formulation are given in the Appendix.

4.2.2 Multiple trains: When there is more than one train on the track, the additional currents drawn by other trains lead to further voltage drop on each conductor and aggregate induced voltages on others. Therefore, the effects of the presence of each train have to be taken into account individually. The train voltage equations can be expressed in a matrix equation as below.

$$\begin{bmatrix} V_{t1} \\ V_{t2} \\ \vdots \\ \vdots \\ V_{tn} \end{bmatrix} = \begin{bmatrix} V_s \\ V_s \\ \vdots \\ \vdots \\ V_s \end{bmatrix} - \begin{bmatrix} Cot_{11} & Cot_{12} & \cdots & \cdots & Cot_{1n} \\ Cot_{21} & Cot_{22} & \cdots & \cdots & Cot_{2n} \\ \vdots & \vdots & \cdots & \cdots & \vdots \\ \vdots & \vdots & \cdots & \cdots & \vdots \\ Cot_{n1} & Cot_{n2} & \cdots & \cdots & Cot_{nn} \end{bmatrix} \begin{bmatrix} \dfrac{P_{t1} - jQ_{t1}}{V_{t1}^*} \\ \dfrac{P_{t2} - jQ_{t2}}{V_{t2}^*} \\ \vdots \\ \vdots \\ \dfrac{P_{tn} - jQ_{tn}}{V_{tn}^*} \end{bmatrix} \qquad (3)$$

where Cot_{ii} is the coefficient of the current of *i*-th train, which is the same as *Cot* in Eqn. (2) and Cot_{ij} $(i \neq j)$ denotes the impedance coefficient of the *j*-th train on the *i*-th one. It should be noted that Cot_{ij}'s are prepared differently if the trains *i* and *j* are not in the same in-feed section as the current distribution differs slightly.

When the real and imaginary parts of the train voltages are extracted separately from Eqn. (3), a set of 2*n* non-linear equations are then available to solve for the unknown voltages. Gauss-Seidel method, with V_{ti}'s set to the rated voltage initially, is an effective method to obtain the solutions. Having known the train voltages, train currents are determined accordingly and hence the total current drawn from the source. The total power demand from the feeding transformer is also established. If the railway line consists of a number of feeding sections, the same process is just repeated in every section.

4.3 BT feeding

Only the single train model is introduced and extension can be made to cater for multi-train as in AT feeding. Similar assumptions are also adopted in the model of BT feeding. There are 3 main conductors along the line, return conductor, catenary and rail, denoted by *f*, *c* and *r* respectively.

It is necessary to consider the two cases with BT feeding when the train is on either side of the nearer contact between *f* and *r*, as illustrated in Figs. 6 and 7. In both cases, train voltage V_t is solved by simultaneous equations in which the coefficients are determined by the train position and feeding system characteristics. Mathematical formulation can be found in the Appendix.

4.4 Direct Feeding

Current distribution with direct feeding is straight-forward as there are two conductors, catenary (*c*) and rails (*r*), providing the feeding and return paths for current, as shown in Fig. 8. Train voltage V_t is again related to train power and feeding system characteristics in simultaneous equations, as devised in the Appendix.

5. Results and Discussions

5.1 Set-up

The PLF model with different feeding systems has been evaluated by computer simulation. The train position pdf's are obtained from speed profiles of station-to-station runs, which are the results from a general-purpose train system simulation suite [25]. Typical track layout and traction equipment characteristics are adopted to generate the speed profiles over a number of stations. The software program to establish the equations shown in the Appendix and the subsequent formulation of solutions through numerical methods in Monte Carlo simulation have been developed with C++ and run on Pentium 4, 2.4GHz PC. Inevitably, the resulting pdf's of train voltage, active and reactive power at the feeding points are of prime interest in load flow analysis. It should be noted that some of the resulting pdf's shown here, particularly those with a dominating component, have been scaled down in order to illustrate the probability distribution in general.

Despite the available data on train voltage and power variations under different traffic conditions from railway operators, they are not in the form of pdf's and hence it is impossible to verify the results from this study directly. In order to deduce the validity of the PLF, the results from different feeding system configurations, traffic demands and operational conditions are compared and analysed. Besides, the necessary sample sizes for Monte Carlo simulation and the corresponding computational demand are also examined.

5.2 Single Feeding Section with ATs

5.2.1 Single Train: The study starts with the simple test of one train running in one AT feeding section with 2 ATs 12km apart and 3 stations. The supply voltage is 55kV (i.e. 2 x 27.5kV) and the feeding point is at one end of the section. The train does not possess regenerative braking capability. Fig. 9a-c illustrates the pdf's of train voltage, active and reactive power at the feeding point.

The pdf shows the train voltage does not rise beyond 27.5kV, which clearly indicates that regenerative braking is not allowed and the train spends more time at station, coasting or braking than motoring. Besides, there is a strong probability around 27.4kV, indicating that the auxiliary power keeps the train voltage slightly lower than the nominal value.

A total of 5,000 random samples have been taken for Monte Carlo simulation and the computation time is only 2 secs. Tests with more samples have also been undertaken and the resulting pdf's are highly similar.

5.2.2 Multiple Trains: 5 trains with headway distance of 3km are running in an AT feeding section covering 36km and 8 stations. There are 4 ATs and they are 12 km apart. The feeding point is next to the second AT. All trains are capable of regenerative braking. Figs. 10 and 11 show the pdf's of the first train and the active power pdf at the feeding point.

With regenerative braking, the train voltage pdf spreads on either side of 27.5kV, so does the power pdf on 0W. Evidently, the probability of train voltage below 27.5kV is higher than that of above and the probability of positive feeding power demand is higher than that of negative. It implies that, in addition to the effects of auxiliary power, energy returned from regenerative braking does not always find a receiving end and hence certain power input is still necessary to get the trains going.

While there are more trains in the system, PLF calculation becomes more tedious. 5,000 samples have been taken to assemble the pdf's and the computation time is 23 secs, which is significantly longer than that in the single-train case but is still reasonable from practical viewpoint.

5.2.3 Traffic demands: Effect of different traffic demands on load flow has been investigated by applying different headway distances on the trains. The identical track and feeding system used in the previous section is adopted for simple comparison. The pdf's of voltage of the first train and the active power at the feeding point are shown in Figs. 12 and 13 respectively.

From the results, it is clear that the pdf of power demand in the case of longer headway tends to spread over a wider range while the train voltage variation is similar. Given that the train separation is longer, it is less likely that the returned energy from regenerative braking of one train can find a motoring train nearby. When the disposed energy during regenerative braking is not efficiently re-cycled within the feeding section, which implies trains may be motoring simultaneously, the peak demand rises as a result.

5.3 Different Feeding Systems

In order to verify the PLF models from the characteristics of the feeding systems, the three feeding systems are applied to the same test-track and traffic conditions and the load flow calculation is undertaken with the proposed PLF models, followed by comparisons of the resulting pdf's.

There are two feeding sections, A and B, over the 36km test-track and they are of equal length. The feeding points are in the middle of the sections and two-way traffic is supported. Six trains are running on tracks with three each direction and regenerative braking is allowed on all trains. The configuration of the test-track is shown in Fig. 14. The headway distances are 3km and 4km in sections A and B respectively. 5 ATs and 7 BTs are adopted in the respective feeding systems and they are evenly located over the line. As the feeding sections are electrically isolated, the PLF calculation is carried out in each section independently in turn. 10,000 samples of train position are taken for Monte Carlo simulation and the results are illustrated in Figs 15-17.

Train voltage variation with AT feeding is clearly smaller as ATs are supposed to provide better voltage regulation. Direct feeding seems to give slightly better voltage regulation than BT feeding does. However, it has to be noted that the assumption of no rail-to-earth leakage current is the least valid for direct feeding. The load flow model thus does not fully reveal the actual current distribution in direct feeding system.

The power demand pdf's are similar among the feeding systems because power demand is mainly determined by the traffic demand rather than the configurations of feeding systems. Despite different headways adopted in the two feeding sections, the feeding systems give similar power demand pdf's as the numbers of trains in the two sections are mostly the same.

5.4.1 BT and AT Separations: Separations among BTs and ATs in the feeding systems impose certain impacts on voltage regulation and effectiveness of electromagnetic interference reduction. In this test, BTs and ATs are separated by different distances over one feeding section of 36km on which four trains with regenerative braking capability are running. The feeding point is at one end, instead of the mid-point, of the section to make any voltage variation more evident. The probabilities of the voltages over the range 26-29kV on trains 1 and 3 and two fixed points on the catenary, N1 and N2, 12km and 20km from the feeding point respectively, are given in Tables 1 and 2.

AT feeding system is overwhelmingly superior in term of voltage regulation. Shorter separation certainly helps improve voltage regulation with AT feeding while it is not obvious with BT feeding. The voltage variation is usually more volatile when it is measured farther from the feeding point (e.g. comparing voltages at N1 and N2). AT feeding however provides a smaller voltage fluctuation even for N2, which is further illustrated in the following section.

5.4.2 Feeding Section Length: The three feeding systems are given different section lengths in this test, 18km and 36km. Three trains are running on the track and the feeding point is in the middle of the section. The probabilities of voltage range 26-29kV of the first train are listed in Table 3. From the results, AT feeding is clearly more suitable for longer section lengths. In other words, it maintains good voltage regulation over longer stretch of track, which is one of its fundamental advantages.

5.5 Conductor Interruption

Broken conductors along the line usually implies a complete breakdown of power supply in direct and BT feeding. However, power supply survives certain conductor interruption with AT feeding despite overloading at the ATs nearby. This section examines this property of AT feeding under broken feeder and rail through PLF calculation in order to further verify the PLF model.

5.5.1 Broken Feeder: In an AT feeding section of 36km, there are 4 ATs and 3 trains running. The feeding point is at one end of the section and a feeder interruption is introduced at 15 km from the feeding point. Fig. 18a-b gives the catenary voltage pdf of the AT nearby with and without the broken feeder whilst Fig. 19a-b shows the respective power demand pdf at the feeding point. Even though the AT is close to the broken feeder point, its catenary voltage pdf is very similar, only slightly dispersed, to that of the normal condition to suggest very good voltage regulation. Indeed, the power demand pdf's are even more comparable as feeder fault should not affect power demand if the feeding system is still able to supply the trains.

5.5.2 Broken Rail: The same feeding and traffic configurations apply in this test and there is a rail interruption at 15 km from the feeding point. It should be noted that broken rail could create dangerous rail potentials in a single rail system in practice and this test is only for the purpose of hypothetical study on the load flow calculation. Catenary voltage pdf at the nearby AT and the power demand pdf are illustrated in Fig. 20a-b. Both voltage and power pdf's show insignificant differences to those in the normal case as the rails only carry current between two ATs when a train is the vicinity. With one rail fault, the current can always find a path through another AT and hence overloading it.

6 Conclusions

We have presented a probability load flow study for AC electrified railways. The needs of probabilistic load flow studies have been discussed, followed by consideration of the difficulties of such studies from the supply and load viewpoints. The approach of Monte Carlo simulation has been proposed for the probabilistic study and train position is selected as the primary random variable to lead to the power demand of the train. In order to take into account the current distributions in the supply system, a train voltage model has been developed to formulate a set of non-linear equations for load flow calculation under the three commonly adopted feeding systems, direct, BT and AT.

Despite the lack of real data on voltage and power probabilistic density functions in railway for comparison, the PLF calculation models have been verified through computer simulation, in which voltage and power pdf's are produced under different feeding configurations and traffic demands. A few cases of supply system conductor faults in AT feeding have also been

investigated to check the capability of the model on dealing with abnormal current distribution. The results point to general agreements of the expected properties among the three feeding systems, implying reasonable modelling and calculation. Besides, the tests also demonstrate the possible studies on the supply system through this PLF analysis.

The PLF models can be further extended to include a thorough current distribution consideration. The assumptions may be relaxed, notably the rail-to-earth leakage current, to improve accuracy while maintaining manageable computational demands. The resulting pdf's are useful for other studies as they provide probabilities of certain ranges of voltage and power at specific points of the supply system. Further studies on the relationship between wear and tear of supply system equipment and its levels of usage and loading, and hence maintenance scheduling of the equipment, have been initiated.

7 Acknowledgements

The authors gratefully acknowledge the generous financial support provided by the Research Grant Council of Hong Kong (PolyU 5104/51E). The authors wish to thank the referees for the detailed review on the technical correctness and presentation quality. Their comments certainly helped improve the paper substantially.

8 References

[1] GOODMAN C.J., SIU, L.K. and HO, T.K.: 'A Review of Simulation Models for Railway Systems', International Conf. On Development in Mass Transit Systems, pp. 80-85, 1998.

[2] GOODMAN, C.J., MELLITT, B. and RAMBUKWELLA, N.B.: 'CAE for the Electrical Design of Urban Rail Transit Systems', COMPRAIL 87, pp. 173-193, 1987.

[3] CHAN, W.S.: Whole System Simulator for AC Traction, PhD Thesis, University of Birmingham, 1988.

[4] DIGBY, G. HEWINGS, D.B. and KADHIM, R.J.: 'Simulation of Voltage Controlled Traction Rectifiers on a Medium Voltage AC Distribution System", COMPRAIL 92, pp. 27-37, 1992.

[5] MELLITT, B., GOODMAN, C.J. and ARTHURTON, R.I.M.: 'Simulator for Studying Operational and Power-supply Conditions in Rapid-transit Railways', Proc. IEE, vol. 125, no. 4, pp. 298-303, 1978.

[6] HILL, R.J. and Cevik, I.H.: 'On-line Simulation of Voltage Regulation in Autotransformer-fed AC Electric Railroad Traction Networks', IEEE Trans. on Vehicular Technology, vol. 42, no. 3, pp. 365-372, 1993.

[7] HILL, R.J. and CAI, Y.: 'Simulation of Rail Voltage and Earth Currents in a PC-based DC Traction Power Simulator', Proc. of ELECTOSOFT 93: Software for Electrical Engineering Analysis and Design, pp. 319-326, 1993.

[8] HILL, R.J. and CEVIK, I.H.: 'Parallel Computer Simulation of Autotransformer-fed AC Traction Networks', Joint ASME/IEEE Railroad Conf., pp. 157-164, 1990.

[9] CAI, Y., IRVING, M.R. and CASE, S.H.: 'Modelling and Numerical Solution of Multibranched DC Rail Traction Power Systems', IEE Proc. Electr. Power Appl., vol. 142, no.5, pp. 323-328, 1995.

[10] ASHIYA, M., YASUDA, M. and SONE, S.: 'Evaluation of Power Feeding Systems for Regenerative Trains', COMPRAIL 98, pp. 469-478, 1998.

[11] ECRAN, M.F., FUNG, Y.F., HO, T.K. and CHEUNG, W.L., 'Parallel Linear System Solution and its Application to Railway Power Network Simulation', EURO-PAR 2003 Parallel Processing, Proc. Lecture Notes in Computer Science, 2790: pp. 537-540, 2003.

[12] STEVENSON, W.D.: Elements of Power System Analysis, 4th Edition, McGraw-Hill, 1982.

[13] HILL, R.J.: 'Electric Railway Traction - Part 3 Traction Power Supplies', Power Engineering Journal, pp. 275-286, December, 1994.

[14] TSE, C.T., CHAN, K.L., HO, S.L., CHUNG, C.Y., CHOW, S.C. and LO, W.Y.: 'Effective Load Flow Technique with Non-constant MVA Load for the Hong Kong Mass Transit Railway Urban Lines Power Distribution System', APSCOM, pp. 753-756, 1997.

[15] BORKOWSKA, B., 'Probabilistic Load Flow', IEEE Trans. on PAS, vol. 93, no. 3, pp.752-759, 1974.

[16] ALLAN, R.N. and AL-SHAKARCHI, M.R.G.: 'Probabilistic Techniques in AC Load Flow Analysis', Proc. IEE, vol. 124, no. 2, pp. 154-160, 1977.

[17] HATZIARGYRIOU, N.D. and KARAKATSANIS, T.S.: 'Distribution System Voltage and Reactive Power Control Based on Probabilistic Load Flow Analysis', IEE Proc.-Gen. Trans. & Distrib., vol. 144, no. 4, pp. 363-369, 1997.

[18] HATZIARGYRIOU, N.D. and KARAKATSANIS, T.S.: 'Probabilistic Load Flow for Assessment of Voltage Instability', IEE Proc.-Gen. Trans. & Distrib., vol. 145, no. 2, pp. 196-202, 1998.

[19] SHAO, Z.Y., Auto-Transformer Power Supply System for Electric Railways, PhD Thesis, University of Birmingham, 1988.

[20] JORGENSEN, P., CHRISTENSEN, J.S. and TANDE, J.O.: 'Probabilistic Load Flow Calculation Using Monte Carlo Techniques for Distribution Network with Wind Turbines', 8th International Conference on Harmonics and Quality of Power, pp. 1146-1151, 1998.

[21] ALLAN, R.H., LEITE DA SILVA, A.M. and BURCHETT, R.C.: 'Evaluation Methods and Accuracy in Probabilistic Load Flow Solutions', IEEE Trans. on PAS, vol. 100, pp. 2539-2546, 1981.

[22] PATRA, S. and MISRA, R.B.: 'Probabilistic Load Flow Solution Using Methods of Moments', IEE ASPCOM'93, pp. 922-934, 1993.

[23] LEITE DA SILVA, A.M. and ARIENTI, V.L.: 'Probabilistic Load Flow by a Multilinear Simulation Algorithm', IEE Proc. C, vol. 137, no. 4, pp. 276-282, 1990.

[24] HO, T.K., CHI, Y.L., WANG, J. and LEUNG, K.K.: 'Load Flow in Electrified Railways', 2nd IEE International Conf. on Power Electronics, Machines and Drives, pp. 498-503, 2004.

[25] HO, T.K., MAO, B.H., YUAN, Z.Z., LIU, H.D. and FUNG, Y.F., "Computer Simulation and Modelling in Railway Applications", Computer Physics Communications, vol. 143, no. 1, pp. 1-10, 2002.

9 Appendix

9.1 AT Feeding

From Fig. 5, the two ATs are at the positions *a* and *b* while the train is at point *x*. The distances *oa*, *ax* and *xb* are denoted by α, β and γ respectively and α is assumed to be very small as the feeding transformer is usually located very close to the first AT. Train current I_t and power demand $P_t + jQ_t$ is related by

$$I_t = \frac{P_t - jQ_t}{V_t^*} \qquad \text{(A1)}$$

The two current components, I_1 and I_2, going into the two ATs, are

$$I_1 = \frac{\gamma}{\beta+\gamma} I_t ; \qquad I_2 = \frac{\beta}{\beta+\gamma} I_t \qquad \text{(A2)}$$

At point *x*, train voltage V_t is given by

$$V_t = V_c - V_r \qquad \text{(A3)}$$

Both V_c and V_r can be derived from currents through the catenary and rail, as well as the induced voltages from currents through other conductors.

$$V_c = V_s - 0.5 I_t Z_s - \left[0.5 I_t Z_c \alpha + 0.5 \left(1 + \frac{\gamma}{\beta+\gamma} \right) I_t Z_c \beta - 0.5 I_t Z_{cf} \alpha - \frac{\gamma}{\beta+\gamma} I_t Z_{cr} \beta - 0.5 \frac{\beta}{\beta+\gamma} I_t Z_{cf} \beta \right]$$

$$V_r = \frac{\gamma}{\beta+\gamma} I_t Z_r \beta - 0.5 \left(1 + \frac{\gamma}{\beta+\gamma} \right) I_t Z_{cr} \beta + 0.5 \frac{\beta}{\beta+\gamma} Z_{cf} \beta$$

While α is small to be negligible,

$$V_c = V_s - I_t\left(0.5Z_s + 0.5\frac{\beta+2\gamma}{\beta+\gamma}Z_c\beta - \frac{\gamma\beta}{\beta+\gamma}Z_{cr} - 0.5\frac{\beta^2}{\beta+\gamma}Z_{cf}\right) \quad \text{(A4)}$$

$$V_r = I_t\left(\frac{\gamma\beta}{\beta+\gamma}Z_r - 0.5\frac{\beta+2\gamma}{\beta+\gamma}Z_{cr}\beta + 0.5\frac{\beta^2}{\beta+\gamma}Z_{rf}\right) \quad \text{(A5)}$$

Combining (A3) (A4) and (A5),

$$V_t = V_s - CotI_t \quad \text{(A6)}$$

where

$$Cot = 0.5Z_s + 0.5\frac{\beta+2\gamma}{\beta+\gamma}Z_c\beta - \frac{\gamma\beta}{\beta+\gamma}Z_{cr} - 0.5\frac{\beta^2}{\beta+\gamma}Z_{cf} + \frac{\gamma\beta}{\beta+\gamma}Z_r - 0.5\frac{\beta+2\gamma}{\beta+\gamma}Z_{cr}\beta + 0.5\frac{\beta^2}{\beta+\gamma}Z_{rf}$$

If Cot_r, Cot_i and V_{tr}, V_{ti} are the real and imaginary parts of *Cot* and V_t respectively, Eqn. (A6) can be re-written by replacing I_t with (A1):

$$V_t = V_s - Cot\frac{P_t - jQ_t}{V_t^*} \quad \text{(A7)}$$

$$|V_t|^2 = V_s(V_{tr} - jV_{ti}) - (Cot_r + jCot_i)(P_t - jQ_t) \quad \text{(A8)}$$

By isolating the real and imaginary parts of (A9), the following two equations are then established to solve for V_{tr} and V_{ti}.

$$V_{tr}^2 - V_sV_{tr} + Cot_rP_t + Cot_iQ_t + V_{ti}^2 = 0 \quad \text{(A9)}$$

$$V_{ti} = \frac{Cot_rQ_t}{V_s} - \frac{Cot_iP_t}{V_s} \quad \text{(A10)}$$

Once V_t is known, I_t is derived from (A1) and the voltage on any point along the conductors can be calculated. Train in regenerative braking has its I_t in opposite direction and the same set of equations applies.

9.2 BT Feeding

9.2.1 Case I: From Fig. 6, let $oa = \alpha$, $ax = \beta$ and $xb = \gamma$, at the train position *x*, the train voltage is $V_t = V_c - V_r$. Again, V_c and V_r are formulated from the current through the catenary and rails and the induced voltages from other conductors.

$$V_c = V_s - I_tZ_s - (I_tZ_c\beta - I_tZ_{cf}\beta + V_{BT} + I_tZ_{BT}) - V_{oa} \quad \text{(A11)}$$

$$V_r = I_tZ_{rf}(\alpha+\beta) - I_tZ_{cr}(\alpha+\beta) \quad \text{(A12)}$$

V_{oa} is the voltage drop from the source to point *a*. There may be a few BTs in between and the impedance along is collectively denoted as Z_{oa} so that $V_{oa} = I_t Z_{oa}$. In order to attain V_{BT}, the voltage between *a* and *x*, V_{ax} on the rail is considered.

$$V_{ax} = \beta I_t Z_{cr} - \beta I_t Z_{cf} \tag{A13}$$

On the other hand,

$$\begin{aligned} V_{ax} &= V_{a'b'} - V_{bx} \\ &= \left(I_t Z_f \beta + I_t Z_{cf} \beta - I_t Z_f \gamma + I_t Z_{rf} \gamma + V_{BT} - I_t Z_{BT} \right) + \left(I_t Z_r \gamma + I_t Z_{rf} \gamma \right) \end{aligned} \tag{A14}$$

Combining Eqns. (A13) and (A14),

$$\beta I_t Z_{cr} - \beta I_t Z_{cf} = \left(I_t Z_f \beta + I_t Z_{cf} \beta - I_t Z_f \gamma + I_t Z_{rf} \gamma + V_{BT} - I_t Z_{BT} \right) + \left(I_t Z_r \gamma + I_t Z_{rf} \gamma \right)$$

$$V_{BT} = I_t \left(Z_f (\beta + \gamma) + Z_r \gamma + Z_{cr} \beta - Z_{cf} \beta - Z_{rf} (\beta + 2\gamma) + Z_{BT} \right)$$

$$V_{BT} = I_t C_{BT1} \qquad \text{where } C_{BT1} = Z_f (\beta + \gamma) + Z_r \gamma + Z_{cr} \beta - Z_{cf} \beta - Z_{rf} (\beta + 2\gamma) + Z_{BT} \tag{A15}$$

Substitute V_{BT} in Eqns. (A11) and (A12),

$$V_t = V_s - I_t \left(Z_s + Z_c \beta - Z_{cf} \beta + C_{BT1} + Z_{BT} + Z_{oa} \right) - I_t \left(Z_{rf} - Z_{cr} \right) (\alpha + \beta)$$

$$V_t = V_s - Co_{BT1} \frac{P_t - jQ_t}{V_t^*} \tag{A16}$$

where $Co_{BT1} = \left(Z_s + Z_c \beta - Z_{cf} \beta + C_{BT1} + Z_{BT} + Z_{oa} \right) + \left(Z_{rf} - Z_{cr} \right) (\alpha + \beta)$

9.2.2 Case II: From Fig. 7, $oa = \alpha$, $ab = \beta$ and $bx = \gamma$. Train voltage V_t is attained from the voltages on the catenary and rails at point *x*.

$$V_c = V_s - I_t Z_s - \left(I_t Z_c \beta - I_t Z_{cf} \beta + V_{BT} + I_t Z_{BT} \right) - V_{oa} - \left(I_t Z_c \gamma - I_t Z_{cr} \gamma \right) \tag{A17}$$

$$V_r = I_t \left(Z_r \gamma + Z_{rf} (\alpha + \beta) - Z_{cr} (\alpha + \beta + \gamma) \right) \tag{A18}$$

By equating voltages over *ab* and *a'b'*,

$$V_{BT} = I_t \left(\beta \left(Z_f + Z_{cr} - Z_{cf} - Z_{rf} \right) + Z_{BT} \right) = I_t C_{BT2} \tag{A19}$$

where $C_{BT2} = \beta \left(Z_f + Z_{cr} - Z_{cf} - Z_{rf} \right) + Z_{BT}$

Combining Eqns. (A17), (A18) and (A19), train voltage is

$$V_t = V_s - I_t \begin{pmatrix} Z_s + Z_c (\beta + \gamma) - Z_{cf} \beta - Z_{cr} \gamma + C_{BT2} + Z_{BT} \\ + Z_{oa} + Z_r \gamma + Z_{rf} (\alpha + \beta) - Z_{cr} (\alpha + \beta + \gamma) \end{pmatrix}$$

$$V_t = V_s - Co_{BT2} \frac{P_t - jQ_t}{V_t^*} \tag{A20}$$

where

$$Co_{BT2} = Z_s + Z_c(\beta + \gamma) - Z_{cf}\beta - Z_{cr}\gamma + C_{BT2} + Z_{BT} + Z_{oa} + Z_r\gamma + Z_{rf}(\alpha + \beta) - Z_{cr}(\alpha + \beta + \gamma)$$

9.3 Direct Feeding

From Fig. 8, with $ox = \beta$, train voltage at point *x* for a single train is derived as follows.

$$V_t = V_c - V_r$$

$$V_t = V_s - I_t Z_s - (I_t Z_c \beta - I_t Z_{cr}\beta) - (I_t Z_r \beta - I_t Z_{cr}\beta)$$

$$V_t = V_s - I_t(Z_s + \beta Z_c + Z_r - 2Z_{cr}) \text{ or}$$

$$V_t = V_s - Co_D \frac{P_t - jQ_t}{V_t^*} \qquad \text{where } Co_D = Z_s + \beta Z_c + Z_r - 2Z_{cr} \qquad \text{(A21)}$$

	4km	6km
Train 1	0.2722	0.2700
Train 3	0.2816	0.2793
N1	0.2977	0.2958
N2	0.2643	0.2675

Table 1 Probabilities of voltage between 26-29kV at various points with different BT separations

	9km	18km
Train 1	0.7023	0.6775
Train 3	0.7143	0.6884
N1	0.7541	0.7428
N2	0.7165	0.7132

Table 2 Probabilities of voltage between 26-29kV at various points with different AT separations

	18km	36km
Direct	0.6075	0.5114
BT	0.5846	0.4832
AT	0.9518	0.9113

Table 3 Probabilities of voltage between 26-29kV with different feeding section lengths

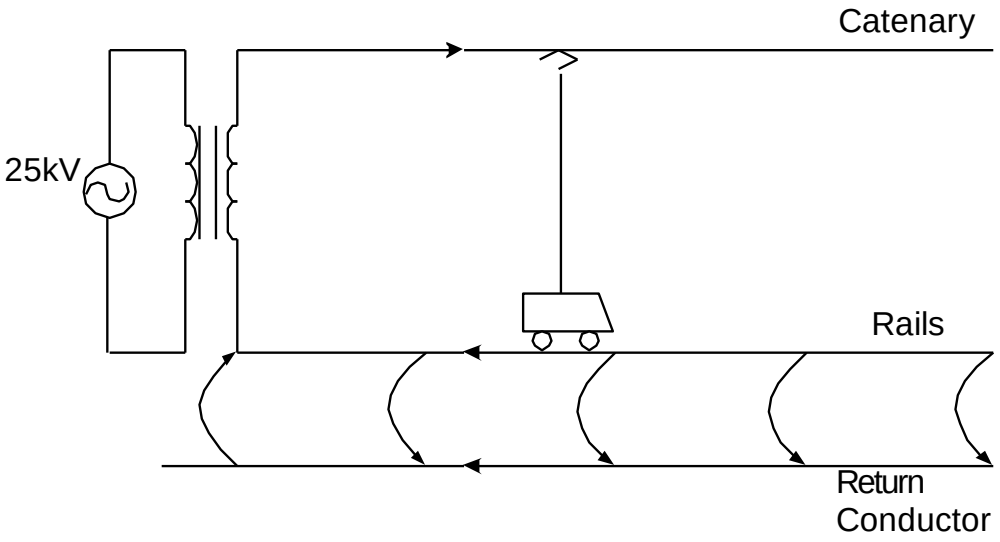

Fig. 1 Direct feeding with return conductor

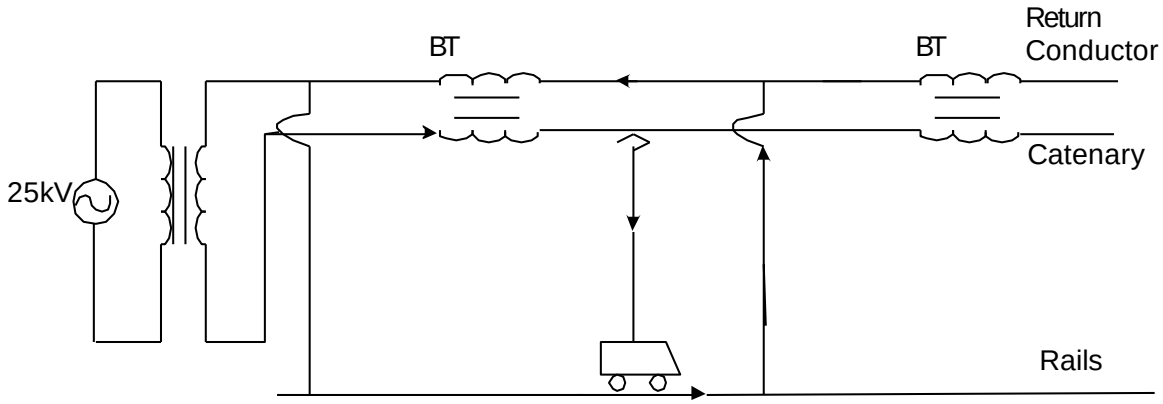

Fig. 2 BT feeding

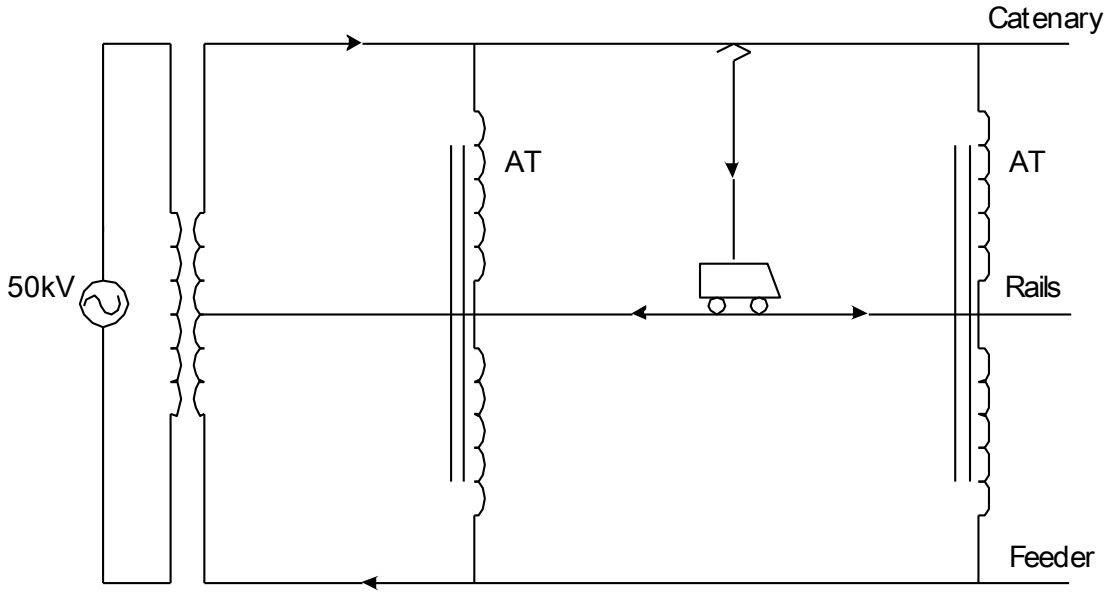

Fig. 3 AT feeding

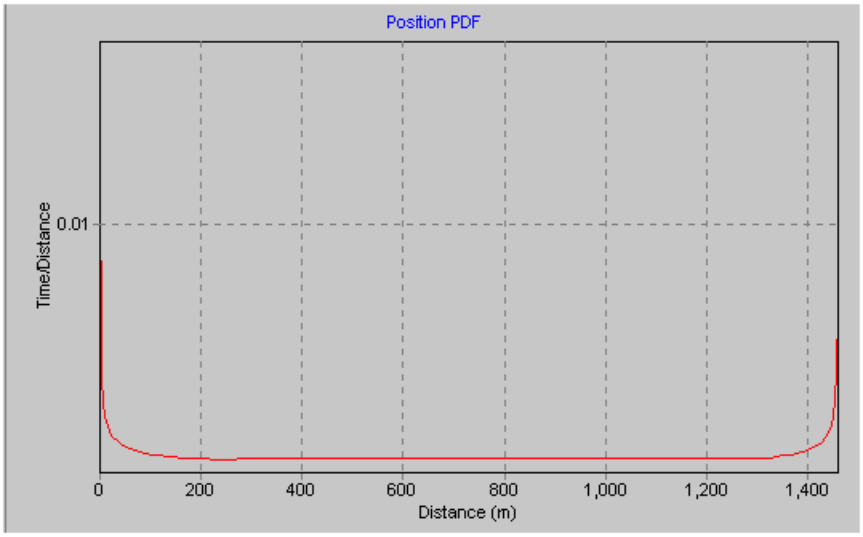

Fig. 4 An example of train position pdf

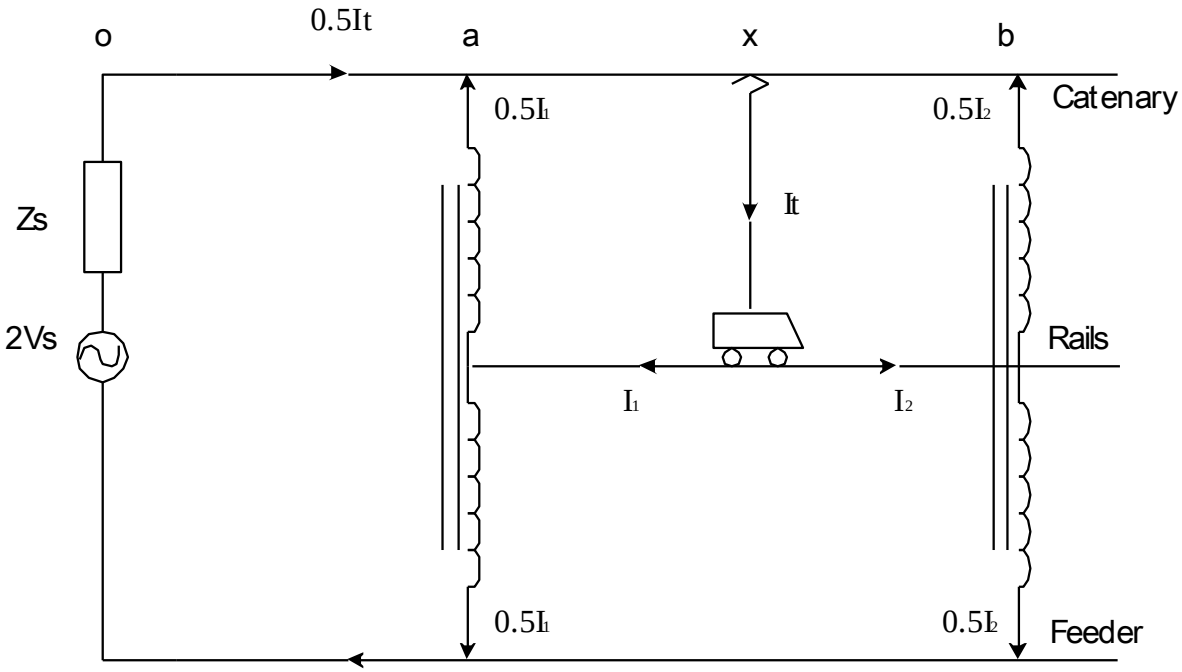

Fig. 5 Current distribution with AT feeding

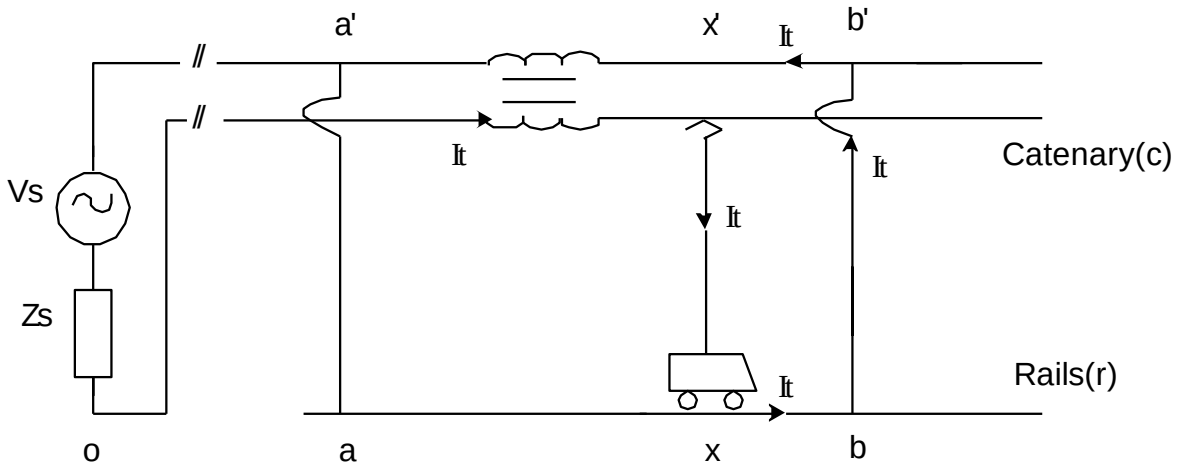

Fig. 6 Current distribution with BT feeding (Case I)

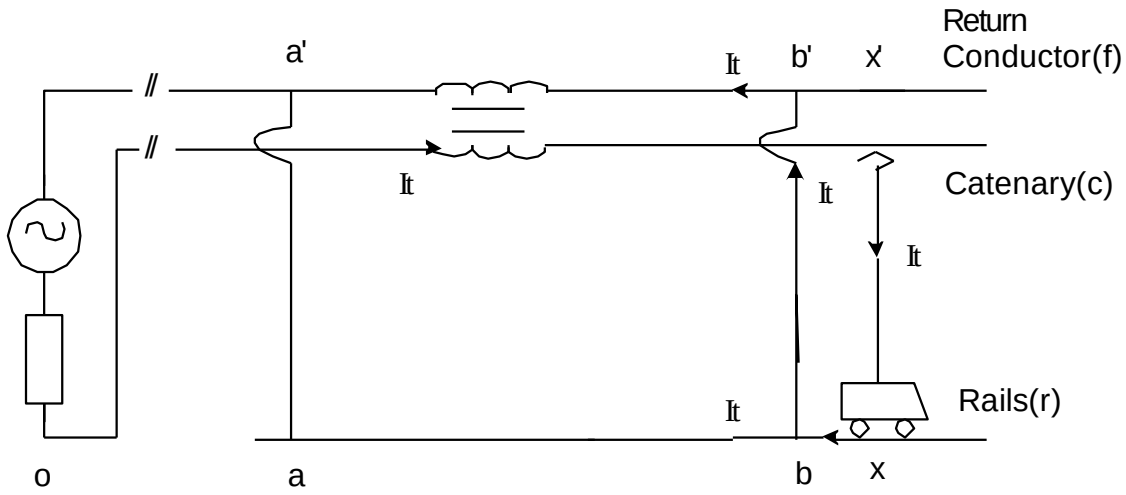

Fig. 7 Current distribution with BT feeding (Case II)

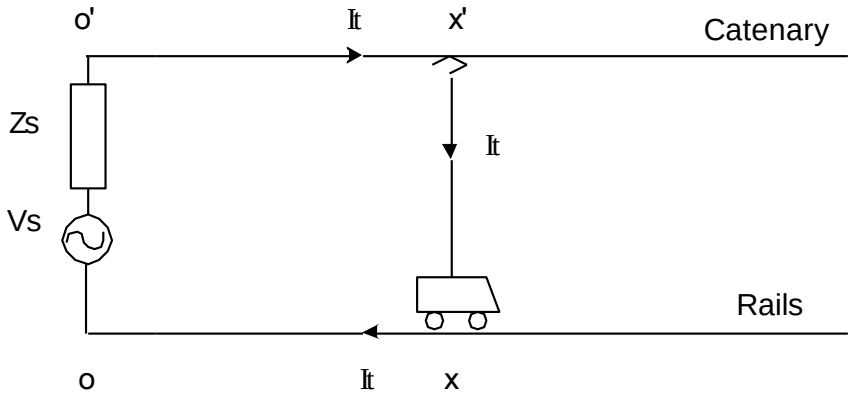

Fig. 8 Current distribution with direct feeding

Fig. 9a Pdf of train voltage (kV)

Fig. 9b Pdf of active power at the feeding point (MW)

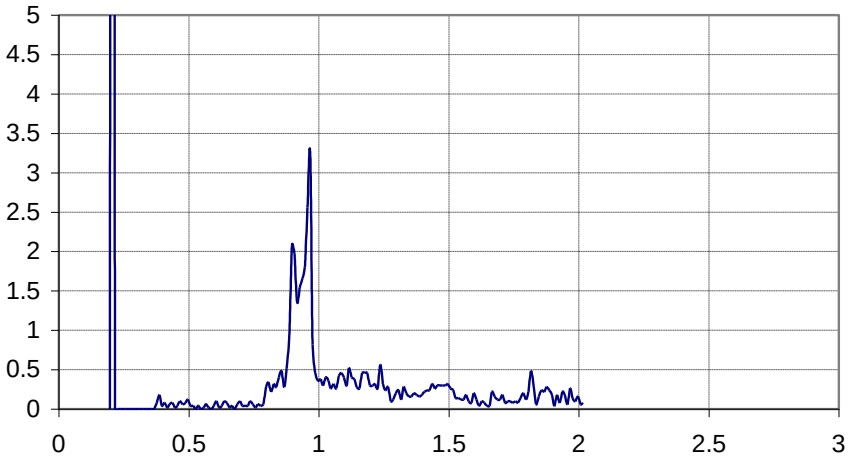

Fig. 9c Pdf of reactive power at the feeding point (MVar)

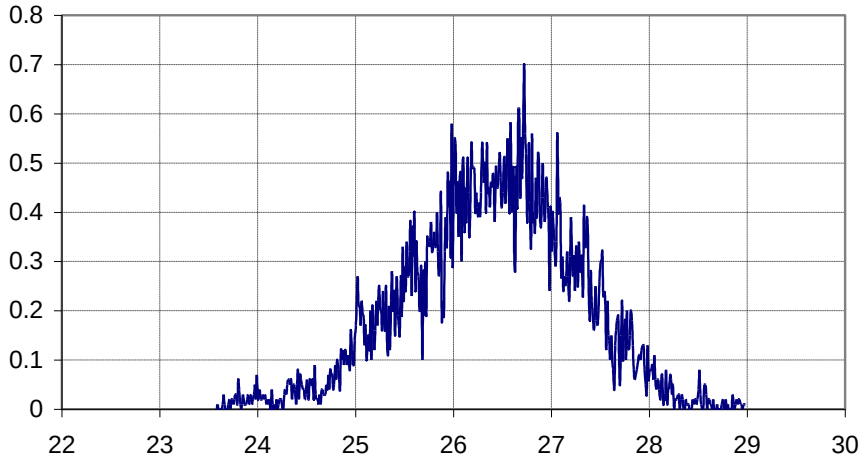

Fig. 10 Voltage pdf of the first train with headway distance 3km

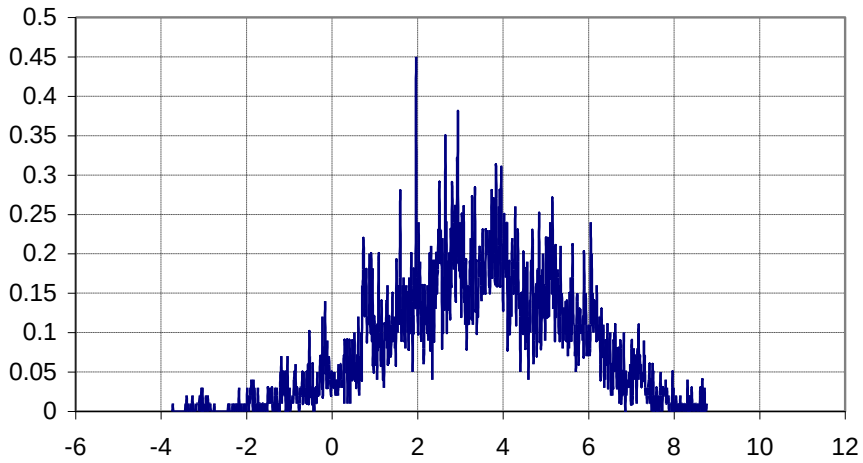

Fig. 11 Pdf of active power at the feeding point with headway distance 3km

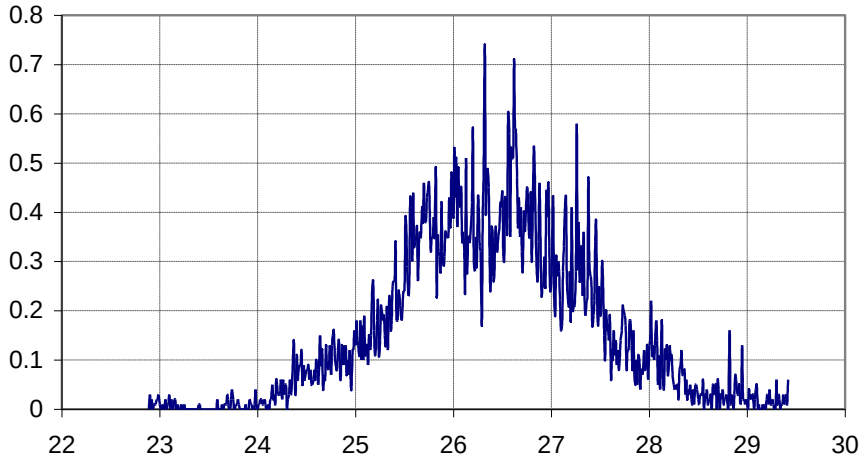

Fig. 12 Voltage pdf of the first train with headway distance 5km

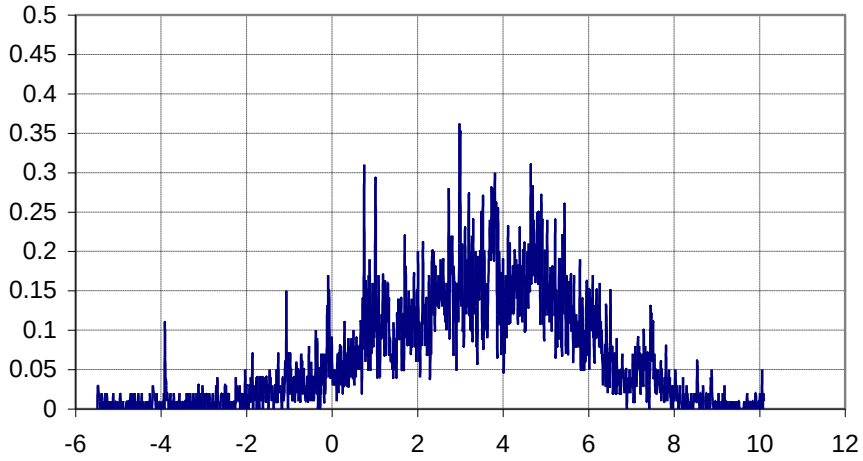

Fig. 13 Pdf of active power at the feeding point with headway distance 5km

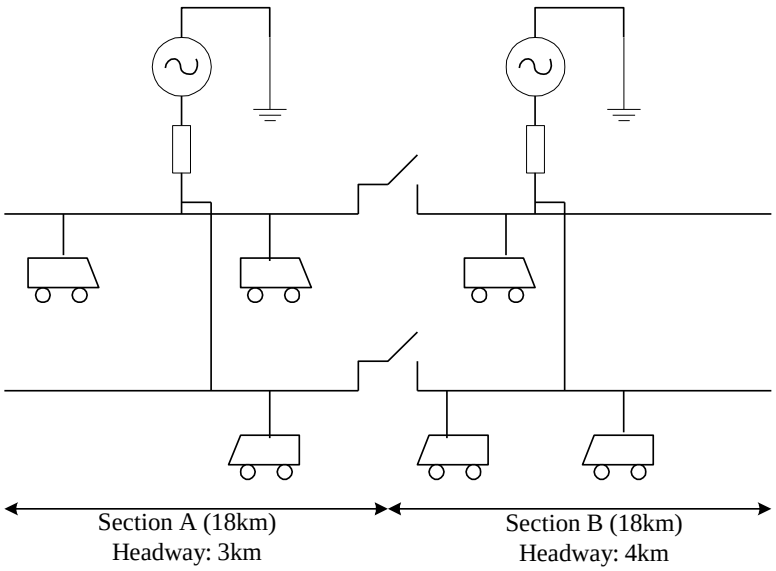

Fig. 14 Configuration of the test-track for studies of different feeding systems

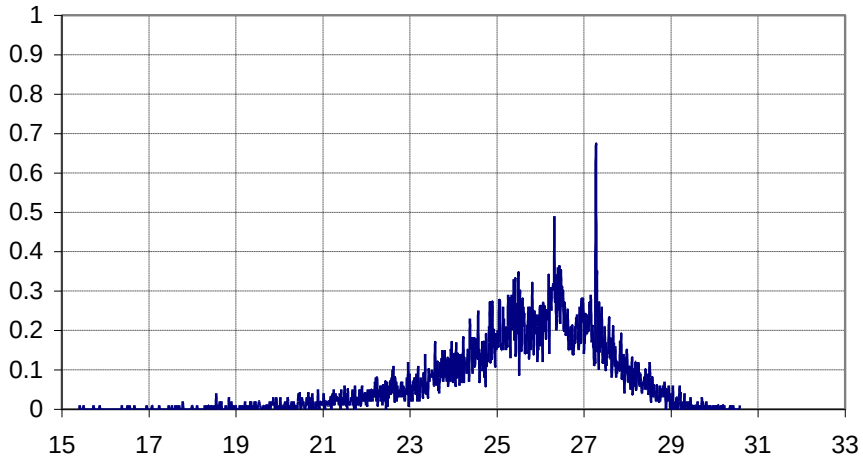

Fig. 15a Voltage pdf of train 1 with direct feeding

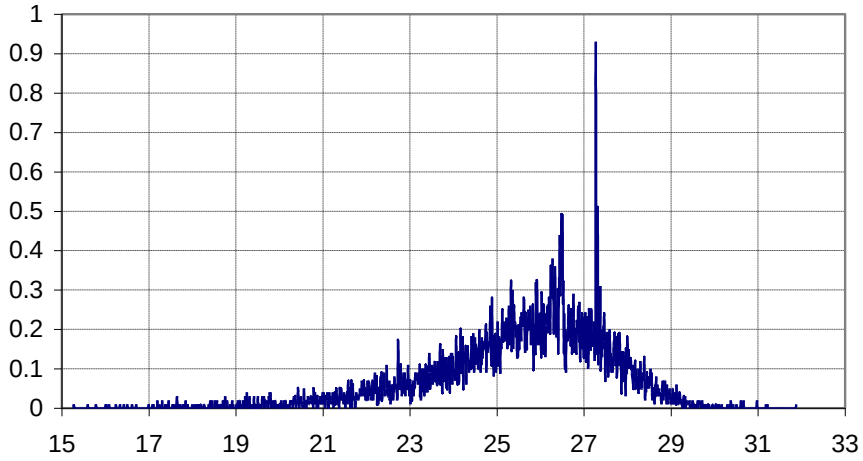

Fig. 15b Voltage pdf of train 1 with BT feeding

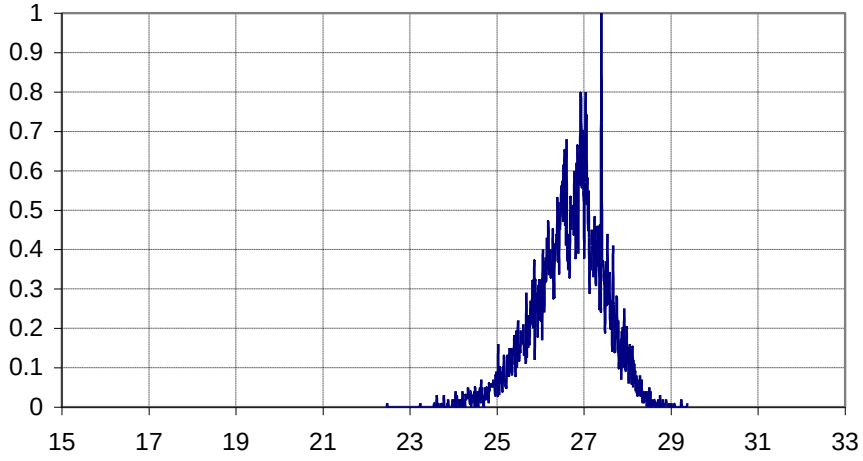

Fig. 15c Voltage pdf of train 1 with AT feeding

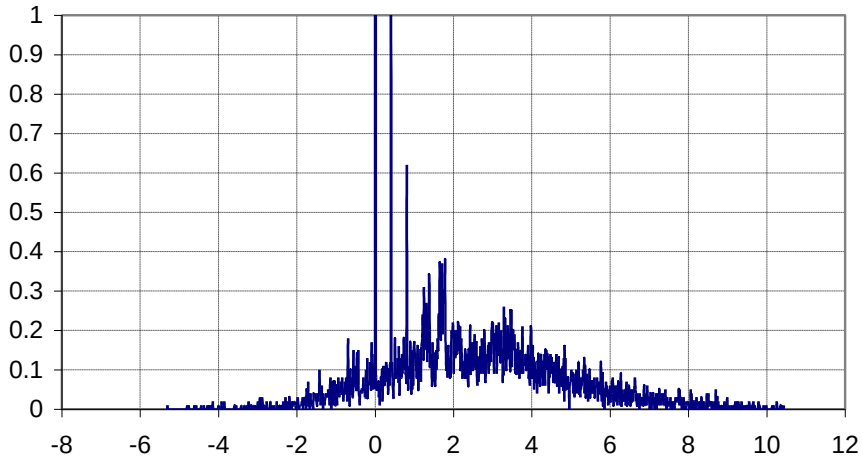

Fig. 16a Active power pdf at the feeding point of the section A with direct feeding

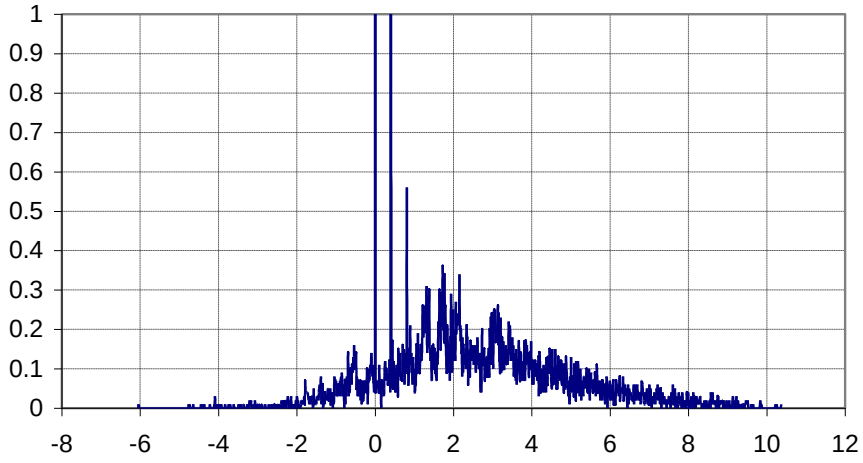

Fig. 16b Active power pdf at the feeding point of the section A with BT feeding

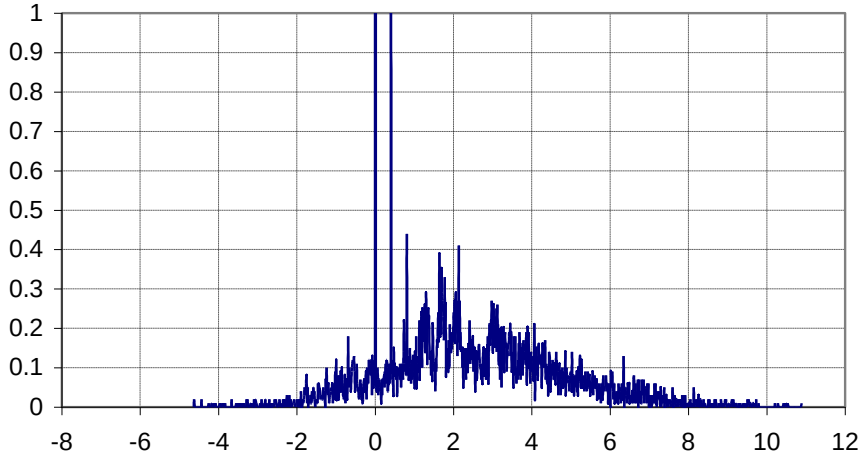

Fig. 16c Active power pdf at the feeding point of the section A with AT feeding

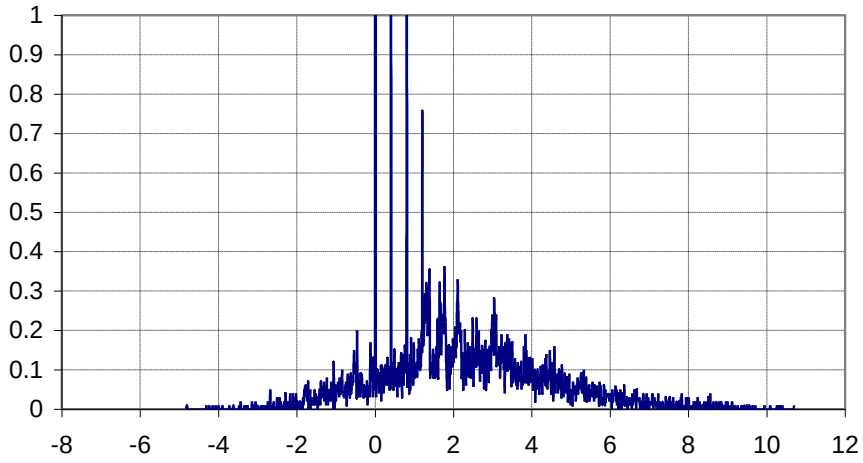

Fig. 17a Active power pdf at the feeding point of the section B with direct feeding

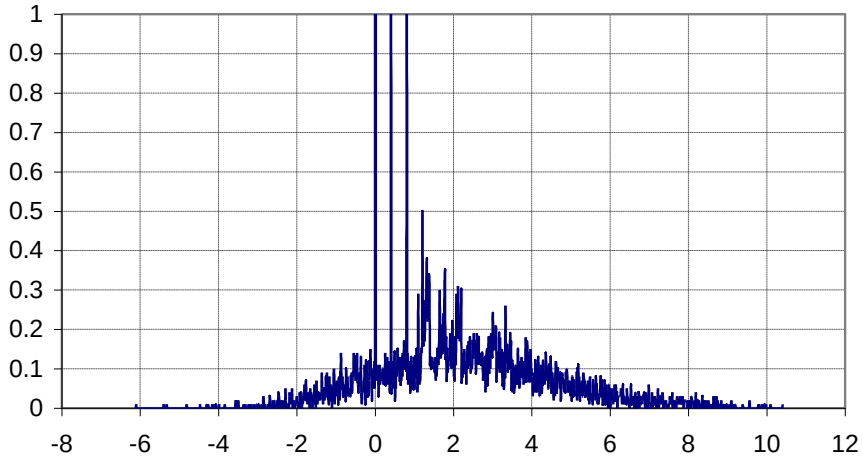

Fig. 17b Active power pdf at the feeding point of the section B with BT feeding

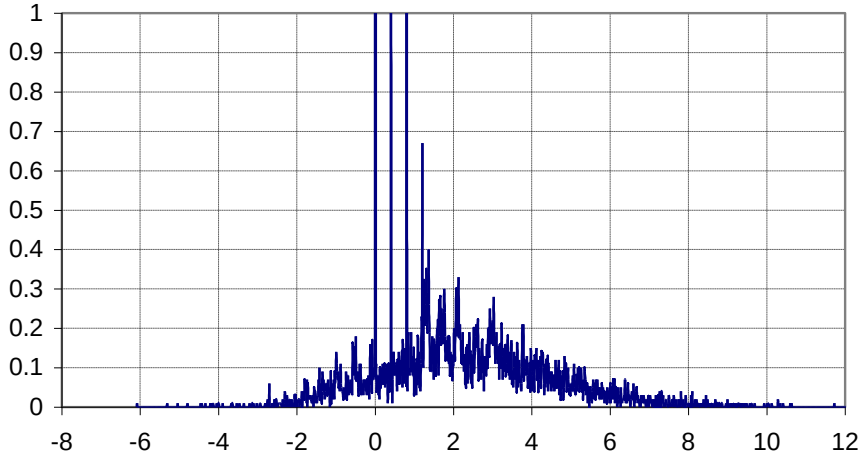

Fig. 17c Active power pdf at the feeding point of the section B with AT feeding

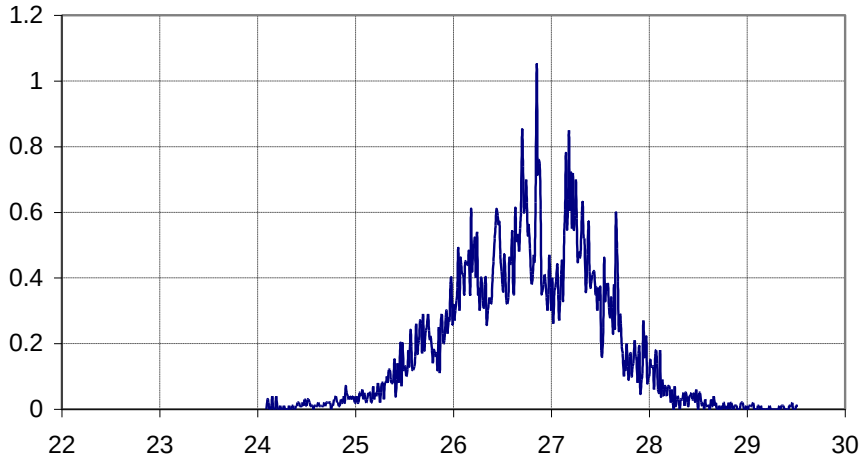

Fig. 18a Catenary voltage pdf at AT without broken feeder

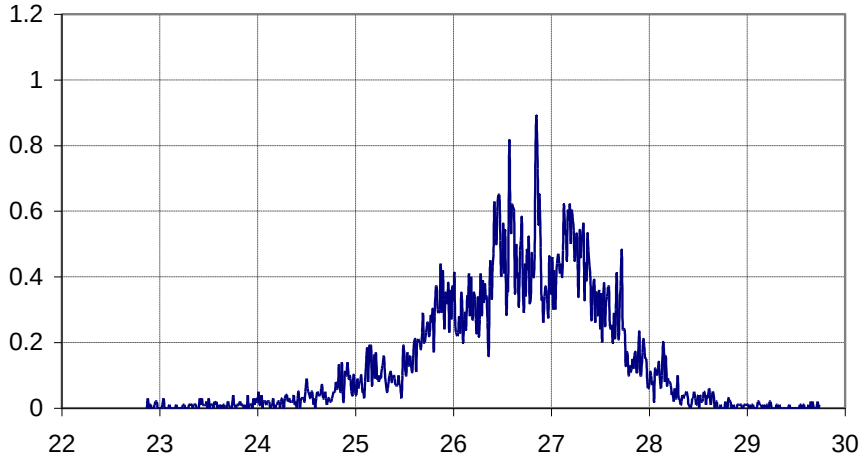

Fig. 18b Catenary voltage pdf at AT with broken feeder

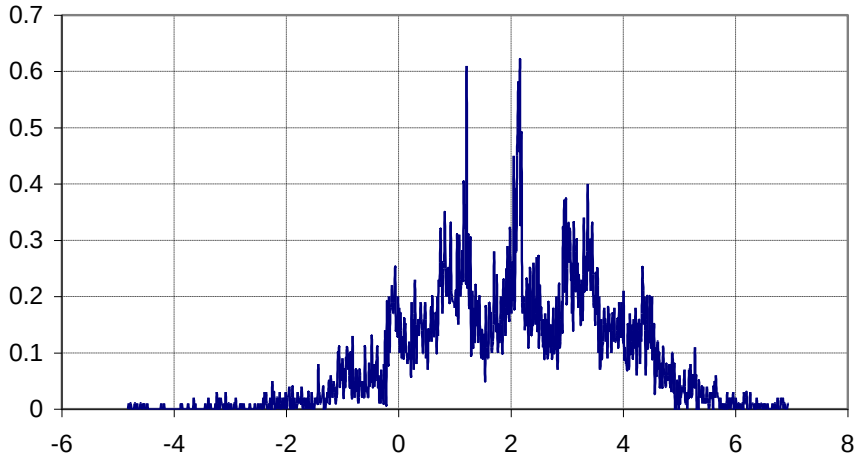

Fig. 19a Power demand pdf without broken feeder

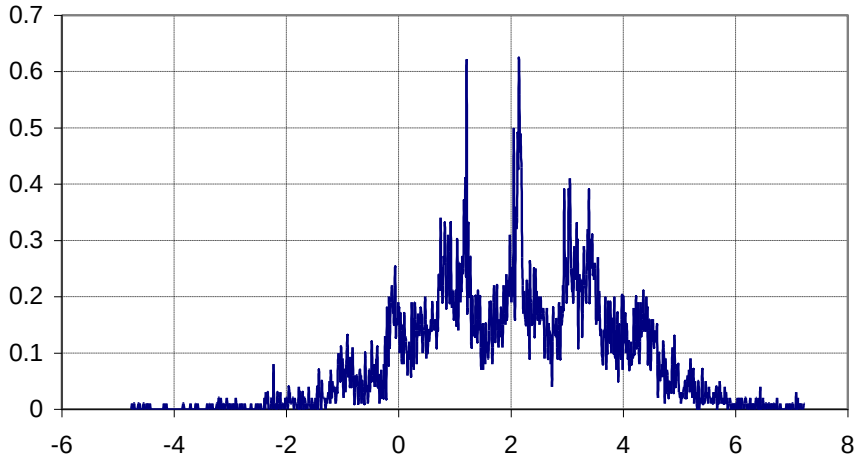

Fig. 19b Power demand pdf with broken feeder

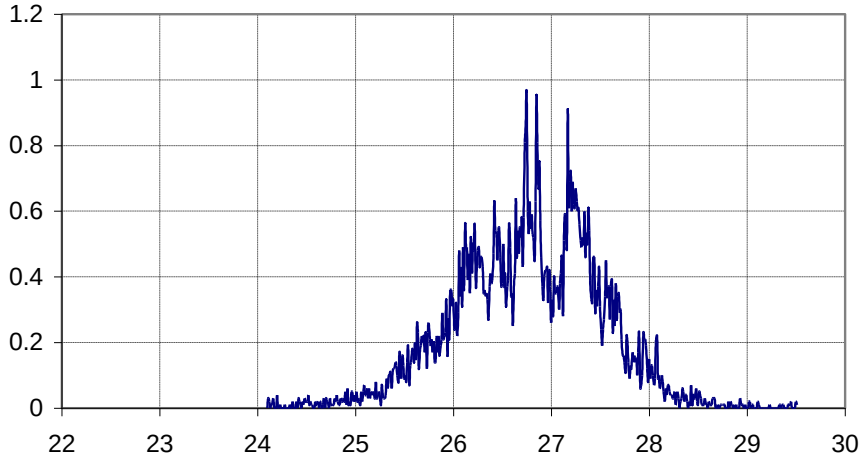

Fig. 20a Catenary voltage pdf at AT with broken rail

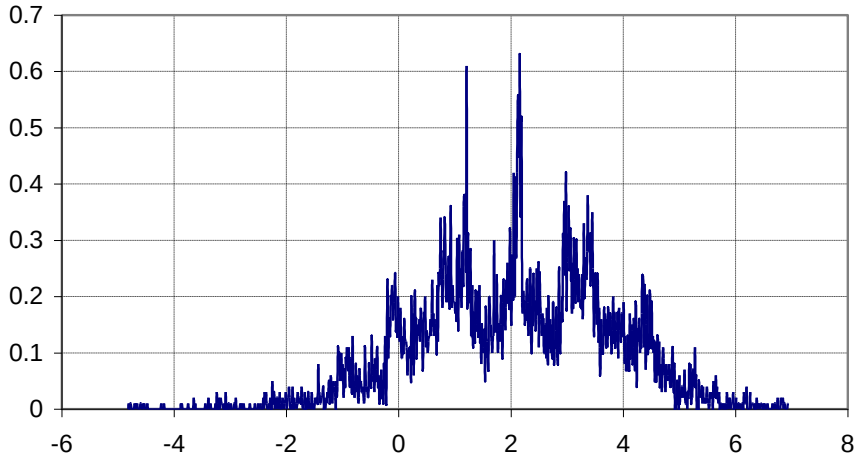

Fig. 20b Power demand pdf with broken rail